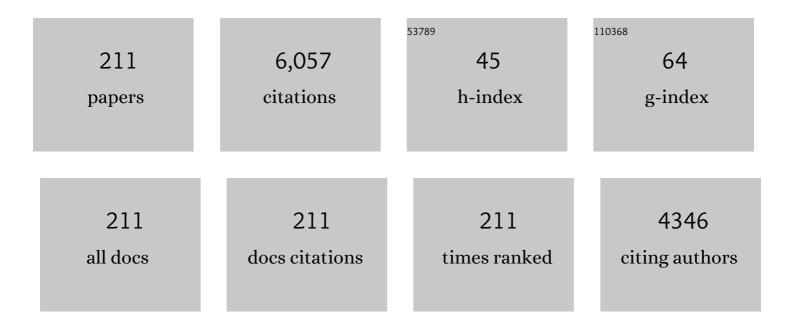
List of Publications by Year in descending order

Source: https://exaly.com/author-pdf/2958963/publications.pdf Version: 2024-02-01



SANTOSH K CUDTA

#	Article	IF	CITATIONS
1	Development of gas sensors using ZnO nanostructures. Journal of Chemical Sciences, 2010, 122, 57-62.	1.5	184
2	A review on molten salt synthesis of metal oxide nanomaterials: Status, opportunity, and challenge. Progress in Materials Science, 2021, 117, 100734.	32.8	153
3	Energy transfer dynamics and luminescence properties of Eu ³⁺ in CaMoO ₄ and SrMoO ₄ . Dalton Transactions, 2015, 44, 18957-18969.	3.3	137
4	Self-assembly of the 3-aminopropyltrimethoxysilane multilayers on Si and hysteretic current–voltage characteristics. Applied Physics A: Materials Science and Processing, 2008, 90, 581-589.	2.3	121
5	Photoluminescence and EPR studies on Fe3+ doped ZnAl2O4: an evidence for local site swapping of Fe3+ and formation of inverse and normal phase. Dalton Transactions, 2014, 43, 9313.	3.3	104
6	An Insight into the Various Defects-Induced Emission in MgAl ₂ O ₄ and Their Tunability with Phase Behavior: Combined Experimental and Theoretical Approach. Journal of Physical Chemistry C, 2016, 120, 4016-4031.	3.1	100
7	Role of various defects in the photoluminescence characteristics of nanocrystalline Nd ₂ Zr ₂ O ₇ : an investigation through spectroscopic and DFT calculations. Journal of Materials Chemistry C, 2016, 4, 4988-5000.	5.5	99
8	Lanthanide-doped lanthanum hafnate nanoparticles as multicolor phosphors for warm white lighting and scintillators. Chemical Engineering Journal, 2020, 379, 122314.	12.7	99
9	Luminescence Properties of SrZrO ₃ /Tb ³⁺ Perovskite: Host-Dopant Energy-Transfer Dynamics and Local Structure of Tb ³⁺ . Inorganic Chemistry, 2016, 55, 1728-1740.	4.0	96
10	Lithium doped zinc oxide based flexible piezoelectric-triboelectric hybrid nanogenerator. Nano Energy, 2019, 61, 327-336.	16.0	88
11	ForceSpun polydiacetylene nanofibers as colorimetric sensor for food spoilage detection. Sensors and Actuators B: Chemical, 2019, 297, 126734.	7.8	87
12	Understanding the local environment of Sm ³⁺ in doped SrZrO ₃ and energy transfer mechanism using time-resolved luminescence: a combined theoretical and experimental approach. RSC Advances, 2014, 4, 29202-29215.	3.6	83
13	Lanthanide spectroscopy in probing structure-property correlation in multi-site photoluminescent phosphors. Coordination Chemistry Reviews, 2020, 420, 213405.	18.8	83
14	Recent Developments on Molten Salt Synthesis of Inorganic Nanomaterials: A Review. Journal of Physical Chemistry C, 2021, 125, 6508-6533.	3.1	83
15	Deciphering the Role of Charge Compensator in Optical Properties of SrWO ₄ :Eu ³⁺ :A (A = Li ⁺ , Na ⁺ , K ⁺): Spectroscopic Insight Using Photoluminescence, Positron Annihilation, and X-ray Absorption. Inorganic Chemistry, 2018, 57, 821-832.	4.0	82
16	Structure and site selective luminescence of sol–gel derived Eu:Sr2SiO4. Journal of Luminescence, 2012, 132, 1329-1338.	3.1	81
17	Intense red emitting monoclinic LaPO ₄ :Eu ³⁺ nanoparticles: host–dopant energy transfer dynamics and photoluminescence properties. RSC Advances, 2015, 5, 58832-58842.	3.6	81
18	Nanospheres, Nanocubes, and Nanorods of Nickel Oxalate: Control of Shape and Size by Surfactant and Solvent. Journal of Physical Chemistry C, 2008, 112, 12610-12615.	3.1	80

#	Article	IF	CITATIONS
19	On the unusual photoluminescence of Eu3+ in α-Zn2P2O7: a time resolved emission spectrometric and Judd–Ofelt study. RSC Advances, 2013, 3, 20046.	3.6	79
20	Eu ³⁺ local site analysis and emission characteristics of novel Nd ₂ Zr ₂ O ₇ :Eu phosphor: insight into the effect of europium concentration on its photoluminescence properties. RSC Advances, 2016, 6, 53614-53624.	3.6	78
21	Defects induced changes in the electronic structures of MgO and their correlation with the optical properties: a special case of electron–hole recombination from the conduction band. RSC Advances, 2016, 6, 96398-96415.	3.6	78
22	An efficient gel-combustion synthesis of visible light emitting barium zirconate perovskite nanoceramics: Probing the photoluminescence of Sm 3+ and Eu 3+ doped BaZrO 3. Journal of Luminescence, 2016, 169, 106-114.	3.1	73
23	Bluish white emitting Sr2CeO4 and red emitting Sr2CeO4:Eu3+ nanoparticles: optimization of synthesis parameters, characterization, energy transfer and photoluminescence. Journal of Materials Chemistry C, 2013, 1, 7054.	5.5	72
24	Experimental and theoretical approach to account for green luminescence from Gd ₂ Zr ₂ O ₇ pyrochlore: exploring the site occupancy and origin of host-dopant energy transfer in Gd ₂ Zr ₂ O ₇ Eu ³⁺ . RSC Advances, 2016, 6, 44908-44920.	3.6	64
25	Multifunctional pure and Eu ³⁺ doped l̂²-Ag ₂ MoO ₄ : photoluminescence, energy transfer dynamics and defect induced properties. Dalton Transactions, 2015, 44, 19097-19110.	3.3	62
26	Correlating Structure and Luminescence Properties of Undoped and Eu ³⁺ -Doped La ₂ Hf ₂ O ₇ Nanoparticles Prepared with Different Coprecipitating pH Values through Experimental and Theoretical Studies. Inorganic Chemistry, 2018, 57, 11815-11830.	4.0	61
27	Thermally Induced Disorder–Order Phase Transition of Gd ₂ Hf ₂ O ₇ Eu ³⁺ Nanoparticles and Its Implication on Photo- and Radioluminescence. ACS Omega, 2019, 4, 2779-2791.	3.5	61
28	Site-specific luminescence of Eu3+ in gel-combustion-derived strontium zirconate perovskite nanophosphors. Journal of Materials Science, 2012, 47, 3504-3515.	3.7	60
29	Exploring the optical properties of La ₂ Hf ₂ O ₇ :Pr ³⁺ nanoparticles under UV and X-ray excitation for potential lighting and scintillating applications. New Journal of Chemistry, 2018, 42, 9381-9392.	2.8	59
30	Nature of defects in blue light emitting CaZrO ₃ : spectroscopic and theoretical study. RSC Advances, 2015, 5, 56526-56533.	3.6	58
31	On structure and phase transformation of uranium doped La ₂ Hf ₂ O ₇ nanoparticles as an efficient nuclear waste host. Materials Chemistry Frontiers, 2018, 2, 2201-2211.	5.9	58
32	Luminescence of undoped and Eu ³⁺ doped nanocrystalline SrWO ₄ scheelite: time resolved fluorescence complimented by DFT and positron annihilation spectroscopic studies. RSC Advances, 2016, 6, 3792-3805.	3.6	57
33	Defect induced ferromagnetism in MgO and its exceptional enhancement upon thermal annealing: a case of transformation of various defect states. Physical Chemistry Chemical Physics, 2017, 19, 11975-11989.	2.8	56
34	Enhanced Photoelectrochemical Water Splitting with Er- and W-Codoped Bismuth Vanadate with WO ₃ Heterojunction-Based Two-Dimensional Photoelectrode. ACS Applied Materials & Interfaces, 2019, 11, 19029-19039.	8.0	56
35	Optical nanomaterials with focus on rare earth doped oxide: A Review. Materials Today Communications, 2021, 27, 102277.	1.9	56
36	ZnO-nanowires modified polypyrrole films as highly selective and sensitive chlorine sensors. Applied Physics Letters, 2009, 94, .	3.3	54

#	Article	IF	CITATIONS
37	Optical properties of sol–gel derived Sr2SiO4:Dy3+ – Photo and thermally stimulated luminescence. Optical Materials, 2013, 35, 2320-2328.	3.6	54
38	Thermal annealing effects on La ₂ Hf ₂ O ₇ :Eu ³⁺ nanoparticles: a curious case study of structural evolution and site-specific photo- and radio-luminescence. Inorganic Chemistry Frontiers, 2018, 5, 2508-2521.	6.0	54
39	Origin of Blue-Green Emission in α-Zn ₂ P ₂ O ₇ and Local Structure of Ln ³⁺ Ion in α-Zn ₂ P ₂ O ₇ :Ln ³⁺ (Ln = Sm,) Tj E 167-178.	TQq1 1 C 4.0	.784314 rg81
40	Interfacial synthesis of long polyindole fibers. Journal of Applied Polymer Science, 2007, 103, 595-599.	2.6	51
41	Probing local site environments and distribution of manganese in SrZrO3:Mn; PL and EPR spectroscopy complimented by DFT calculations. RSC Advances, 2015, 5, 17501-17513.	3.6	51
42	Exploring pure and RE co-doped (Eu3+, Tb3+ and Dy3+) gadolinium scandate: Luminescence behaviour and dynamics of energy transfer. Chemical Engineering Journal, 2016, 283, 114-126.	12.7	51
43	The role of reaction conditions in the polymorphic control of Eu ³⁺ doped YInO ₃ : structure and size sensitive luminescence. Dalton Transactions, 2015, 44, 10628-10635.	3.3	49
44	Photoluminescence Investigations of the Near White Light Emitting Perovskite Ceramic <scp><scp>SrZrO</scp></scp> ₃ : <scp><scp>Dy</scp></scp> ³⁺ Prepared Via Gel ombustion Route. International Journal of Applied Ceramic Technology, 2013, 10, 593-602.	2.1	47
45	Crystallographic site swapping of La ³⁺ ion in BaA′LaTeO ₆ (A′ = Na, K, Rb) double perovskite type compounds: diffraction and photoluminescence evidence for the site swapping. Dalton Transactions, 2014, 43, 3306-3312.	3.3	47
46	Effect of Molten Salt Synthesis Processing Duration on the Photo- and Radioluminescence of UV-, Visible-, and X-ray-Excitable La ₂ Hf ₂ O ₇ :Eu ³⁺ Nanoparticles. ACS Omega, 2018, 3, 7757-7770.	3.5	47
47	Why host to dopant energy transfer is absent in the MgAl ₂ O ₄ Eu ³⁺ spinel? And exploring Eu ³⁺ site distribution and local symmetry through its photoluminescence: interplay of experiment and theory. RSC. Advances, 2016, 6, 42923-42932.	3.6	46
48	Doping-Induced Room Temperature Stabilization of Metastable β-Ag ₂ WO ₄ and Origin of Visible Emission in α- and β-Ag ₂ WO ₄ : Low Temperature Photoluminescence Studies. Journal of Physical Chemistry C, 2016, 120, 7265-7276.	3.1	46
49	Single red emission from upconverting ZnGa ₂ O ₄ :Yb,Er nanoparticles co-doped by Cr ³⁺ . Journal of Materials Chemistry C, 2020, 8, 6370-6379.	5.5	46
50	Origin of blue emission in ThO ₂ nanorods: exploring it as a host for photoluminescence of Eu ³⁺ , Tb ³⁺ and Dy ³⁺ . RSC Advances, 2014, 4, 51244-51255.	3.6	45
51	Role of Synthesis Method on Luminescence Properties of Europium(II, III) Ions in β-Ca2SiO4: Probing Local Site and Structure. Inorganic Chemistry, 2018, 57, 935-950.	4.0	44
52	Samarium-Activated La ₂ Hf ₂ O ₇ Nanoparticles as Multifunctional Phosphors. ACS Omega, 2019, 4, 17956-17966.	3.5	44
53	Optical properties of Eu 3+ activated thorium molybdate and thorium tungstate: Structure, local symmetry and photophysical properties. Journal of Photochemistry and Photobiology A: Chemistry, 2015, 311, 59-67.	3.9	43
54	Optical properties of undoped, Eu ³⁺ doped and Li ⁺ co-doped Y ₂ Hf ₂ O ₇ nanoparticles and polymer nanocomposite films. Inorganic Chemistry Frontiers, 2020, 7, 505-518.	6.0	43

SANTOSH K GUPTA

#	Article	IF	CITATIONS
55	Recent advances, challenges, and opportunities of inorganic nanoscintillators. Frontiers of Optoelectronics, 2020, 13, 156-187.	3.7	42
56	On the photo-luminescence properties of sol–gel derived undoped and Dy3+ ion doped nanocrystalline Scheelite type AMoO4 (A = Ca, Sr and Ba). Materials Research Bulletin, 2015, 64, 223-232.	5.2	41
57	Structural characterization and photoluminescence properties of sol–gel derived nanocrystalline BaMoO4:Dy3+. Journal of Luminescence, 2015, 158, 203-210.	3.1	40
58	Probing Site Symmetry Around Eu ³⁺ in Nanocrystalline ThO ₂ Using Time Resolved Emission Spectroscopy. Journal of the American Ceramic Society, 2014, 97, 3694-3701.	3.8	39
59	On comparison of luminescence properties of La ₂ Zr ₂ O ₇ and La ₂ Hf ₂ O ₇ nanoparticles. Journal of the American Ceramic Society, 2020, 103, 235-248.	3.8	38
60	MgAl2O4 spinel: Synthesis, carbon incorporation and defect-induced luminescence. Journal of Molecular Structure, 2015, 1089, 81-85.	3.6	37
61	Tunable white light emitting Sr 2 V 2 O 7 :Bi 3+ phosphors: Role of bismuth ion. Materials and Design, 2017, 130, 208-214.	7.0	37
62	Performance evaluation of Ce3+ doped flexible PVDF fibers for efficient optical pressure sensors. Sensors and Actuators A: Physical, 2019, 298, 111595.	4.1	37
63	Bright persistent green emitting water-dispersible Zn ₂ GeO ₄ :Mn nanorods. Dalton Transactions, 2020, 49, 7328-7340.	3.3	37
64	Roles of oxygen vacancies and pH induced size changes on photo- and radioluminescence of undoped and Eu3+-doped La2Zr2O7 nanoparticles. Journal of Luminescence, 2019, 209, 302-315.	3.1	36
65	γ-Fe2O3 nanoflowers as efficient magnetic hyperthermia and photothermal agent. Applied Surface Science, 2021, 560, 150025.	6.1	36
66	Visible light emitting Ln3+ ion (Ln=Sm, Eu and Dy) as a structural probe: A case study with SrZrO3. Journal of Luminescence, 2015, 164, 1-22.	3.1	35
67	Europium Luminescence as a Structural Probe: Structure-Dependent Changes in Eu3+-Substituted Th(C2O4)2·xH2O (x= 6, 2, and 0). European Journal of Inorganic Chemistry, 2015, 2015, 4429-4436.	2.0	34
68	Pyrochlore Rare-Earth Hafnate RE ₂ Hf ₂ O ₇ (RE = La and Pr) Nanoparticles Stabilized by Molten-Salt Synthesis at Low Temperature. Inorganic Chemistry, 2019, 58, 1241-1251.	4.0	34
69	Remarkable enhancement of photoluminescence and persistent luminescence of NIR emitting ZnGa ₂ O ₄ :Cr ³⁺ nanoparticles. CrystEngComm, 2020, 22, 2491-2501.	2.6	33
70	Nanoparticles of Sr0.995Gd0.005ZrO3-gel-combustion synthesis, characterization, fluorescence and EPR spectroscopy. Materials Science and Engineering B: Solid-State Materials for Advanced Technology, 2014, 183, 6-11.	3.5	32
71	An insight into local environment of lanthanide ions in Sr ₂ SiO ₄ :Ln (Ln = Sm,) Tj ETQq1	1 0,78431 2.8	4.rgBT /Ove
79	Orange-red emitting Gd2Zr2O7:Sm3+: Structure-property correlation, optical properties and defect	4.0	32

spectroscopy. Journal of Physics and Chemistry of Solids, 2018, 116, 360-366.

#	Article	IF	CITATIONS
73	Revealing the oxidation number and local coordination of uranium in Nd 2 Zr 2 O 7 pyrochlore: A photoluminescence study. Journal of Luminescence, 2016, 177, 166-171.	3.1	30
74	Visible and ultraviolet upconversion and near infrared downconversion luminescence from lanthanide doped La2Zr2O7 nanoparticles. Journal of Luminescence, 2019, 214, 116591.	3.1	30
75	Role of alkali charge compensation in the luminescence of CaWO ₄ :Nd ³⁺ and SrWO ₄ :Nd ³⁺ Scheelites. New Journal of Chemistry, 2020, 44, 7300-7309.	2.8	30
76	Radiation effects on SBR–EPDM blends: A correlation with blend morphology. Journal of Polymer Science, Part B: Polymer Physics, 2006, 44, 1676-1689.	2.1	29
77	Bias and temperature dependent charge transport in high mobility cobalt-phthalocyanine thin films. Applied Physics Letters, 2010, 96, .	3.3	29
78	Probing the oxidation state and coordination geometry of uranium ion in SrZrO3 perovskite. Journal of Molecular Structure, 2014, 1068, 204-209.	3.6	29
79	The effect of vanadium substitution on photoluminescent properties of KSrLa(PO ₄) _x (VO ₄) _{2â^'x} :Eu ³⁺ phosphors, a new variant of phosphovanadates. New Journal of Chemistry, 2016, 40, 1799-1806.	2.8	29
80	Defect evolution in Eu ³⁺ , Nb ⁵⁺ doped and co-doped CeO ₂ : X-ray diffraction, positron annihilation lifetime and photoluminescence studies. Inorganic Chemistry Frontiers, 2019, 6, 2167-2177.	6.0	29
81	A Novel near white light emitting nanocrystalline Zn2P2O7:Sm3+ derived using citrate precursor route: Photoluminescence spectroscopy. Advanced Powder Technology, 2014, 25, 1388-1393.	4.1	28
82	Warm white light emitting ThO2:Sm3+ nanorods: Cationic surfactant assisted reverse micellar synthesis and Photoluminescence properties. Materials Research Bulletin, 2014, 49, 297-301.	5.2	28
83	Energy transfer dynamics and time resolved photoluminescence in BaWO4:Eu3+ nanophosphors synthesized by mechanical activation. New Journal of Chemistry, 2017, 41, 8947-8958.	2.8	28
84	Speciation of uranium and doping induced defects in Gd1.98U0.02Zr2O7: Photoluminescence, X-ray photoelectron and positron annihilation lifetime spectroscopy. Chemical Physics Letters, 2017, 669, 245-250.	2.6	26
85	Evidence for the stabilization of manganese ion as Mn (II) and Mn (IV) in α-Zn2P2O7: Probed by EPR, luminescence and electrochemical studies. Materials Chemistry and Physics, 2014, 145, 162-167.	4.0	25
86	Local site symmetry of Sm3+ in sol–gel derived α′-Sr2SiO4: Probed by emission and fluorescence lifetime spectroscopy. Journal of Luminescence, 2016, 169, 669-673.	3.1	25
87	An insight into optical spectroscopy of intense green emitting ZnAl2O4:Tb3+ nanoparticles: photo, thermally stimulated luminescence and EPR study. Journal of Luminescence, 2015, 168, 151-157.	3.1	24
88	Li+ co-doping induced phase transition as an efficient strategy to enhance upconversion of La2Zr2O7:Er,Yb nanoparticles. Journal of Luminescence, 2020, 224, 117312.	3.1	24
89	MgAl2O4 both as short and long persistent phosphor material: Role of antisite defect centers in determining the decay kinetics. Solid State Sciences, 2019, 88, 13-19.	3.2	23
90	Direct dissolution of uranium oxides in deep eutectic solvent: An insight using electrochemical and luminescence study. Journal of Molecular Structure, 2020, 1215, 128266.	3.6	22

SANTOSH K GUPTA

#	Article	IF	CITATIONS
91	Oxygen induced hysteretic current-voltage characteristics of iron-phthalocyanine thin films. Journal of Applied Physics, 2008, 104, .	2.5	21
92	Near white light emitting ZnAl2O4:Dy3+ nanocrystals: Sol–gel synthesis and luminescence studies. Materials Research Bulletin, 2016, 74, 182-187.	5.2	21
93	Visible light emission from bulk and nano SrWO4: Possible role of defects in photoluminescence. Journal of Luminescence, 2017, 192, 1220-1226.	3.1	21
94	Structural evolution and giant magnetoresistance in electrodeposited Co-Cu/Cu multilayers. Physical Review B, 2008, 77, .	3.2	20
95	Understanding the Dynamics of Eu ³⁺ Ions in Roomâ€Temperature Ionic Liquids – Electrochemical and Timeâ€Resolved Fluorescence Spectroscopy Studies. European Journal of Inorganic Chemistry, 2015, 2015, 104-111.	2.0	20
96	Yellow Emission from Low Coordination Site of Sr ₂ SiO ₄ :Eu ²⁺ , Ce ³⁺ : Influence of Lanthanide Dopants on the Electron Density and Crystallinity in Crystal Site Engineering Approach. Chemistry - A European Journal, 2018, 24, 16149-16159.	3.3	20
97	Defect-induced optical and electrochemical properties of Pr ₂ Sn ₂ O ₇ nanoparticles enhanced by Bi ³⁺ doping. Journal of Materials Research, 2020, 35, 1214-1224.	2.6	20
98	Nanorods of white light emitting Sr ₂ SiO ₄ :Eu ²⁺ : microemulsion-based synthesis, EPR, photoluminescence, and thermoluminescence studies. Journal of Experimental Nanoscience, 2015, 10, 610-621.	2.4	19
99	Size, structure, and luminescence of Nd2Zr2O7 nanoparticles by molten salt synthesis. Journal of Materials Science, 2019, 54, 12411-12423.	3.7	19
100	High pressure induced local ordering and tunable luminescence of La ₂ Hf ₂ O ₇ :Eu ³⁺ nanoparticles. New Journal of Chemistry, 2020, 44, 5463-5472.	2.8	19
101	Molten‣altâ€Assisted Annealing for Making Colloidal ZnGa ₂ O ₄ :Cr Nanocrystals with High Persistent Luminescence. Chemistry - A European Journal, 2021, 27, 11398-11405.	3.3	19
102	Tunable CsPb(Br/Cl) ₃ perovskite nanocrystals and further advancement in designing light emitting fiber membranes. Materials Advances, 2021, 2, 2700-2710.	5.4	19
103	Role of surface defects in catalytic properties of CeO 2 nanoparticles towards oxygen reduction reaction. Materials Chemistry and Physics, 2017, 200, 99-106.	4.0	18
104	Room temperature synthesis, concentration quenching study and defect formation in β-Ag2MoO4:Dy3+- photoluminescence and positron annihilation spectroscopy. Journal of Luminescence, 2019, 212, 293-299.	3.1	18
105	A carnegieite type red emitting NaAlSiO4:Eu3+ phosphor: Concentration dependent time resolved photoluminescence and Judd-Ofelt analysis. Journal of Luminescence, 2019, 209, 283-290.	3.1	18
106	High pressure responsive luminescence of flexible Eu3+ doped PVDF fibrous mats. Journal of Materials Science and Technology, 2021, 66, 103-111.	10.7	17
107	Charge transport in polypyrrole:ZnO-nanowires composite films. Applied Physics Letters, 2009, 95, 202106.	3.3	16
108	On the photophysics and speciation of actinide ion in MgAl2O4 spinel using photoluminescence spectroscopy and first principle calculation: A case study with uranium. Journal of Alloys and Compounds, 2017, 695, 337-343.	5.5	16

#	Article	IF	CITATIONS
109	Solid state speciation of uranium and its local structure in Sr2CeO4 using photoluminescence spectroscopy. Spectrochimica Acta - Part A: Molecular and Biomolecular Spectroscopy, 2018, 195, 113-119.	3.9	16
110	Insight into the effect of A-site cations on structural and optical properties of RE2Hf2O7:U nanoparticles. Journal of Luminescence, 2019, 210, 425-434.	3.1	16
111	Effects of molten-salt processing parameters on the structural and optical properties of preformed La2Zr2O7:Eu3+ nanoparticles. Ceramics International, 2020, 46, 1352-1361.	4.8	16
112	Achieving Bright Blue and Red Luminescence in Ca ₂ SnO ₄ through Defect and Doping Manipulation. Journal of Physical Chemistry C, 2020, 124, 16090-16101.	3.1	16
113	Electrochemical and thermodynamic insights on actinide type (IV) deep eutectic solvent. Journal of Molecular Liquids, 2021, 329, 115550.	4.9	16
114	Harvesting Light from BaHfO ₃ /Eu ³⁺ through Ultraviolet, X-ray, and Heat Stimulation: An Optically Multifunctional Perovskite. ACS Omega, 2022, 7, 5311-5323.	3.5	16
115	Speciation and site occupancy of uranium in strontium orthosilicate by photoluminescence and X-ray absorption spectroscopy: A combined experimental and theoretical approach. Spectrochimica Acta - Part A: Molecular and Biomolecular Spectroscopy, 2015, 151, 453-458.	3.9	15
116	Appearance of new photoluminescence peak and spectral evolution of Eu3+ in La2Zr2O7 nanoparticles at high pressure. Journal of Alloys and Compounds, 2021, 870, 159438.	5.5	15
117	Temperature dependent electron paramagnetic resonance (EPR) of SrZrO. Journal of Magnetism and Magnetic Materials, 2015, 391, 101-107.	2.3	14
118	Unraveling doping induced anatase–rutile phase transition in TiO ₂ using electron, X-ray and gamma-ray as spectroscopic probes. Physical Chemistry Chemical Physics, 2018, 20, 28699-28711.	2.8	14
119	Defect and dopant induced photoluminescence of molten salt synthesized BaZrO3 crystals. Journal of Luminescence, 2019, 214, 116599.	3.1	14
120	Color tuning in CaZrO3:RE3+ perovskite by choice of rare earth ion. Journal of Molecular Structure, 2020, 1221, 128776.	3.6	14
121	Influence of Li+ co-doping on the luminescence of MgO:Eu3+ nanocrystals: Probing asymmetry, energy transfer and defects. Solid State Sciences, 2020, 105, 106286.	3.2	14
122	Electrochemical, Thermodynamic and Spectroscopic Investigations of Celllin a 1-Ethyl-3-methylimidazolium Ethyl Sulfate (EMIES) Ionic Liquid. European Journal of Inorganic Chemistry, 2015, 2015, 4396-4401.	2.0	13
123	Effect of Oxide Ion Distribution on a Uranium Structure in Highly U-Doped RE ₂ Hf ₂ O ₇ (RE = La and Gd) Nanoparticles. Inorganic Chemistry, 2020, 59, 14070-14077.	4.0	13
124	Rare earth free bright and persistent white light emitting zinc gallo-germanate nanosheets: technological advancement to fibers with enhanced quantum efficiency. Materials Advances, 2021, 2, 4058-4067.	5.4	13
125	Multiphoton light emission in barium stannate perovskites driven by oxygen vacancies, Eu ³⁺ and La ³⁺ : accessing the role of defects and local structures. Physical Chemistry Chemical Physics, 2021, 23, 17479-17492.	2.8	13
126	Influence of sulphur atom on the qualitative behavior of electron impact total cross sections of some sulphur containing molecules. Indian Journal of Physics, 2011, 85, 1717-1720.	1.8	12

#	Article	IF	CITATIONS
127	Origin of visible photoluminescence in combustion synthesized α-Al 2 O 3 : Photoluminescence and EPR spectroscopy. Advanced Powder Technology, 2017, 28, 1505-1510.	4.1	12
128	Investigating the impact of gamma radiation on structural and optical properties of Eu3+ doped rare-earth hafnate pyrochlore nanocrystals. Journal of Luminescence, 2019, 207, 1-13.	3.1	12
129	Luminescent PVDF nanocomposite films and fibers encapsulated with La2Hf2O7:Eu3+ nanoparticles. SN Applied Sciences, 2020, 2, 1.	2.9	12
130	Up- and Down-Convertible LaF ₃ :Yb,Er Nanocrystals with a Broad Emission Window from 350 nm to 2.8 μm: Implications for Lighting Applications. ACS Applied Nano Materials, 2021, 4, 13562-13572.	5.0	12
131	Resistive memory effect in selfâ€assembled 3â€aminopropyltrimethoxysilane molecular multilayers. Physica Status Solidi (A) Applications and Materials Science, 2008, 205, 373-377.	1.8	11
132	Dopant Concentration induced optical changes in Ba 1â^'x Eu x MoO 4 : A green and facile approach towards tunable photoluminescent material. Journal of Luminescence, 2017, 188, 67-74.	3.1	11
133	Redox and Photophysical Behaviour of Complexes of NpO2+ Ions with Carbomyl methyl phosphine oxide in 1-Hexyl-3-methylimidazolium bis (trifluoromethylsulfonyl) imide Ionic Liquid. Electrochimica Acta, 2017, 224, 269-277.	5.2	11
134	Bright and persistent green and red light-emitting fine fibers: A potential candidate for smart textiles. Journal of Luminescence, 2021, 231, 117760.	3.1	11
135	Inversion in usual excitation intensities from solid state phosphor and improved fluorescence of Eu3+ ion in type (IV) deep eutectic solvent. Journal of Luminescence, 2021, 235, 118026.	3.1	11
136	Light Harvesting from Oxygen Vacancies and A- and B-Site Dopants in CaSnO ₃ Perovskite through Efficient Photon Utilization and Local Site Engineering. ACS Applied Electronic Materials, 2021, 3, 3256-3270.	4.3	11
137	Europium luminescence as a structural probe to understand defect evolution in CeO2/Eu3+, M3+ (M = Y) ŢjĘTQq1	$\frac{1}{10.7843}$
138	Positron annihilation studies in theMgB2superconductor. Physical Review B, 2002, 66, .	3.2	10
139	Growth and morphology of the single crystals of thermoelectric oxide material NaxCoO2. Crystal Research and Technology, 2004, 39, 572-576.	1.3	10
140	Tunneling characteristics and resistivity behavior ofLa0.6Pb0.4MnO3grain boundaries. Physical Review B, 2006, 73, .	3.2	10
141	White light emission from co-doped La ₂ Hf ₂ O ₇ nanoparticles with suppressed host → Eu ³⁺ energy transfer <i>via</i> a U ⁶⁺ co-dopant. Inorganic Chemistry Frontiers, 2021, 8, 3830-3842.	6.0	10
142	Multifunctional delafossite CuFeO2 as water splitting catalyst and rhodamine B sensor. Materials Chemistry and Physics, 2022, 278, 125643.	4.0	10
143	Photoacoustic spectroscopy of Ln3+ (Nd, Ho, and Er) doped ThO2. Journal of Molecular Structure, 2013, 1051, 95-100.	3.6	9
144	EPR investigation on synthesis of Lithium zinc vanadate using sol–gel-combustion route and its optical properties. Journal of Molecular Structure, 2014, 1056-1057, 121-126.	3.6	9

#	Article	IF	CITATIONS
145	Optical properties of ammonium uranyl fluoride characterized by photoluminescence and photoacoustic spectroscopy. Spectrochimica Acta - Part A: Molecular and Biomolecular Spectroscopy, 2014, 117, 204-209.	3.9	9
146	Probing local coordination and oxidation state of uranium in ThO2: UÂnanostructured. Journal of Molecular Structure, 2015, 1102, 81-85.	3.6	9
147	pH induced size tuning of Gd2Hf2O7:Eu3+ nanoparticles and its effect on their UV and X-ray excited luminescence. Journal of Luminescence, 2020, 228, 117605.	3.1	9
148	Probing emission and defects in BaW _x Mo _{1–x} O ₄ solid solutions: achieving color tunable luminescence by W/Mo ratio and size manipulation. New Journal of Chemistry, 2020, 44, 10380-10389.	2.8	9
149	Tetragonal ZrO2:Nd3+ nanosphere: Combustion synthesis, luminescence and photoacoustic spectroscopy. Journal of Molecular Structure, 2015, 1102, 141-145.	3.6	8
150	A novel self activated K2XV2O7 (XÂ=ÂMg and Zn) pyrovanadate green phosphor: Systematic characterization and time resolved photoluminescence. Solid State Sciences, 2016, 61, 207-214.	3.2	8
151	Excitation dependent site-specific luminescence and structure-optical property correlation of Lu2Sn2O7:Eu3+ nanoparticles. Optical Materials, 2020, 109, 110357.	3.6	8
152	Defect engineering in trivalent ion doped ceria through vanadium assisted charge compensation: insight using photoluminescence, positron annihilation and electron spin resonance spectroscopy. Dalton Transactions, 2021, 50, 17378-17389.	3.3	8
153	Structural Changes from Conventional SrSnO ₃ to Ruddlesden–Popper Sr ₂ SnO ₄ Perovskites and Its Implication on Photoluminescence and Optoelectronic Properties. ACS Applied Electronic Materials, 2022, 4, 878-890.	4.3	8
154	Crystal structure of Ba ₂ (La _{0.727} Ba _{0.182} M _{0.091})MO ₆ (M = Nb,) T Transactions, 2017, 46, 1694-1703.	j ETQq0 0	0 rgBT /Overl
155	On high purity fullerenol obtained by combined dialysis and freeze-drying method with its morphostructural transition and photoluminescence. Separation and Purification Technology, 2019, 210, 927-934.	7.9	7
156	Role of energy transfer, defect, and lattice dimension in photophysical characteristics of AWO ₄ :Nd ³⁺ (A=Ca, Sr and Ba). Journal of the American Ceramic Society, 2020, 103, 5098-5110.	3.8	7
157	Achieving blue emission via f→d transition from pyrochlore Eu2+ and Ce3+-doped La2Zr2O7 nanoparticles. Journal of Molecular Structure, 2020, 1220, 128688.	3.6	7
158	MnFe2O4 nano-flower: A prospective material for bimodal hyperthermia. Journal of Alloys and Compounds, 2022, 899, 163192.	5.5	7
159	Stabilization of UO22+ in SrHfO3 perovskite and probing defects, local structure and photo/thermoluminescence. Journal of Luminescence, 2022, 243, 118663.	3.1	7
160	Dopant-Free, Blue-Light-Emitting, Hydrophobic Deep Eutectic Solvent and Its Application as a Liquid Scintillator. ACS Applied Electronic Materials, 2022, 4, 2175-2179.	4.3	7
161	Effect of Na2O/K2O substitution on thermophysical properties of PbO based phosphate glasses. Journal of Thermal Analysis and Calorimetry, 2007, 89, 153-157.	3.6	6
162	Unusual magnetic properties of Mn-doped ThO ₂ nanoparticles. Journal of Materials Research, 2008, 23, 463-472.	2.6	6

#	Article	IF	CITATIONS
163	Molten-Salt Synthesis of Complex Metal Oxide Nanoparticles. Journal of Visualized Experiments, 2018, , \cdot	0.3	6
164	A step towards synthesizing unique UV and visible light excitable AWO4:Eu3+ (A = Ca and Sr) nanophosphors using high energy ball milling method: luminescence differences in going from Ca2+ → Sr2+. Journal of Materials Science: Materials in Electronics, 2018, 29, 13751-13765.	2.2	6
165	Pressure-induced site swapping, luminescence quenching, and color tunability of Gd2Hf2O7:Eu3+ nanoparticles. Optical Materials, 2021, 112, 110789.	3.6	6
166	Enhanced sensitivity of caterpillar-like ZnO nanostructure towards amine vapor sensing. Materials Research Bulletin, 2021, 142, 111419.	5.2	6
167	Efficient near infrared to visible light upconversion from Er/Yb codoped PVDF fibrous mats synthesized using a direct polymer doping technique. Optical Materials, 2022, 123, 111866.	3.6	6
168	Modulating the optical and electrical properties of oxygen vacancy-enriched La ₂ Ce ₂ O ₇ :Sm ³⁺ pyrochlore: role of dopant local structure and concentration. New Journal of Chemistry, 2022, 46, 4353-4362.	2.8	6
169	In-plane and out-of-plane anisotropic magnetoresistances in La1 â^'xPbxMnO3thin films. Philosophical Magazine, 2003, 83, 3181-3191.	1.6	5
170	Probing structural evolution in thorium–cerium mixed oxides thermally annealed in oxidizing and reducing conditions. Journal of Nuclear Materials, 2020, 539, 152344.	2.7	5
171	Doped lanthanum cerate pyrochlore for multicolor luminescent phosphor: Decisive role of energy transfer and defects. Journal of Luminescence, 2021, 236, 118072.	3.1	5
172	Light emission of Lu2Sn2O7 pyrochlore driven by oxygen vacancy and local site engineering. Journal of Alloys and Compounds, 2022, 893, 162249.	5.5	5
173	Thickness dependent morphology and resistivity of ultra-thin Al films grown on Si(111) by molecular beam epitaxy. Physica Status Solidi (A) Applications and Materials Science, 2006, 203, 1254-1258.	1.8	4
174	Novel Electrochemical Synthesis of Polypyrrole/Ag Nanocomposite and Its Electrocatalytic Performance towards Hydrogen Peroxide Reduction. Journal of Nanoparticles, 2015, 2015, 1-6.	1.4	4
175	Oxidation state determination of uranium in various uranium oxides: Photoacoustic spectroscopy complimented by photoluminescence studies. Journal of Molecular Structure, 2015, 1084, 89-94.	3.6	4
176	Singular orange emission in Zn2SnO4:Eu3+. Materials Letters, 2020, 279, 128511.	2.6	4
177	Controlling the luminescence in K2Th(PO4)2:Eu3+ by energy transfer and excitation photon: a multicolor emitting phosphor. New Journal of Chemistry, 2020, 44, 14703-14711.	2.8	4
178	Structural Evolution and Magnetic Properties of Gd2Hf2O7 Nanocrystals: Computational and Experimental Investigations. Molecules, 2020, 25, 4847.	3.8	4
179	Bright aspects of defects and dark traits of dopants in the photoluminescence of Er ₂ X ₂ O ₇ :Eu ³⁺ (X = Ti and Zr) pyrochlore: an insight using EXAFS, positron annihilation and DFT. Materials Advances, 2021, 2, 3075-3087.	5.4	4
180	Cr3+ assisted energy transfer for Mn2+ doped zinc gallogermanate with narrow and bright green emission. Materials Letters, 2021, 297, 129964.	2.6	4

#	Article	IF	CITATIONS
181	Photophysical Properties of Eu(III) in Zirconia Nanocrystals Derived via Microemulsion Route from Oxalate Precursor. Advanced Science, Engineering and Medicine, 2014, 6, 667-675.	0.3	4
182	Redox and emission characteristics of Eu3+ in deep eutectic solvent: Unraveling the hidden potential of DES as luminescent media. Journal of Molecular Structure, 2022, 1251, 132000.	3.6	4
183	Resistivity behaviour of ultra thin Pd films with respect to temperature for sensing applications. , 0, , .		3
184	Structural phase transition in Zn _{1.98} Mn _{0.02} P ₂ O ₇ : EPR evidence for enhanced line broadening and large zero-field splitting parameter in high temperature phase. Journal of Materials Research, 2013, 28, 3157-3163.	2.6	3
185	Disorder driven asymmetry and singular red emission in doped Lu2Hf2O7 nanocrystals with no charge compensating defects. Journal of Luminescence, 2021, 235, 118057.	3.1	3
186	High pressure induced disappearing 5D0 → 7F2 and broadening 5D0 → 7F1 transitions from Y2Hf2O7:Eu3+ nanoparticles. Materials Letters, 2021, 303, 130560.	2.6	3
187	Photon energy dependent appearance and disappearance of magnetic dipole transition in Gd2Hf2O7:Sm3+ nanophosphors. Journal of Luminescence, 2022, 245, 118789.	3.1	3
188	Suppressing disorder-order phase transition of Gd2Zr2O7 pyrochlore by Dy3+ doping and their impact on luminescence. Materials Today Chemistry, 2022, 24, 100931.	3.5	3
189	Achieving tunable luminescence in rare earth free IRMOF-3 through post synthetic modifications by judicious choice of organic linker. Optical Materials, 2022, 131, 112660.	3.6	3
190	H₂S DETECTION BY CuO NANOWIRES AT ROOM TEMPERATURE. International Journal of Nanoscience, 2011, 10, 733-737.	0.7	2
191	Novel synthesis and characterization of nanocrystalline thoria from oxalate precursor via reverse micellar route. Radiochimica Acta, 2013, 101, 7-12.	1.2	2
192	Oxidation state of manganese in zinc pyrophosphate: Probed by luminescence and EPR studies. , 2014, , .		2
193	A MODULAR-TYPE ATOMIC ABSORPTION INSTRUMENT WITH THE GRAPHITE FURNACE IN A GLOVE BOX FOR NUCLEAR APPLICATIONS. Instrumentation Science and Technology, 2014, 42, 161-172.	1.8	2
194	Photoacoustic and photoluminescence studies on ThO2:Sm3+. Journal of Radioanalytical and Nuclear Chemistry, 2017, 313, 547-553.	1.5	2
195	Ultraviolet emission and electron spin characteristics of Th(C2O4)2·xH2O:Gd3+. New Journal of Chemistry, 2020, 44, 16036-16044.	2.8	2
196	Effect of hydrothermal temperature treatment on the variance of fluorescence in Ca2SiO4:Tb3+. Journal of Science: Advanced Materials and Devices, 2020, 5, 250-255.	3.1	2
197	Morphology-oxygen evolution activity relationship of iridium(<scp>iv</scp>) oxide nanomaterials. New Journal of Chemistry, 2022, 46, 3716-3726.	2.8	2
198	Probing defect-originated properties, actinide-lanthanide doping, and gamma irradiation effect in Lu2Hf2O7 pyrochlore nanocrystals for phosphor and nuclear applications. Materials Today Chemistry, 2022, 23, 100761.	3.5	2

#	Article	IF	CITATIONS
199	Preparation and characterization of MgB2 superconductor. Pramana - Journal of Physics, 2002, 58, 867-870.	1.8	1
200	Effect of substrate temperature on electrical and magnetic properties of epitaxial La1â^'x Pb x MnO3 films. Pramana - Journal of Physics, 2002, 58, 1065-1067.	1.8	1
201	Colossal magnetoresistance in layered manganite Nd2â^'2x Sr1+2x Mn2O7 (0 ≤ ≤0.5). Pramana - Journal of Physics, 2002, 58, 1085-1088.	1.8	1
202	Molecular Beam Epitaxy Growth of Iron Phthalocyanine Nanostructures. , 2009, , .		1
203	Ab-initio study of oxygen defects in pure ThO2. AIP Conference Proceedings, 2016, , .	0.4	1
204	Ultraviolet, blue and singular green upconversion from Gd2Hf2O7 nanocrystals through dopant manipulation. Solid State Communications, 2021, 338, 114458.	1.9	1
205	Synergistic effect of doping and defect in achieving white light emission and oxygen reduction catalysis in Ce1-xSmxPO4. Materials Today Chemistry, 2022, 25, 100947.	3.5	1
206	Anomalous temperature dependence of resistance observed for high T _C Y-Ba-Cu-O thin films. Phase Transitions, 1989, 18, 125-130.	1.3	0
207	Microwave absorption studies of MgB2 superconductor. Pramana - Journal of Physics, 2002, 58, 799-802.	1.8	0
208	Study of SnO/sub 2/ and SnO/sub 2/:CuO thin films for H/sub 2/S gas sensing applications. , 0, , .		0
209	Growth Mechanism of Zinc Oxide Nanostructures by Carbothermal Evaporation Technique. , 2009, , .		0
210	Study of H[sub 2]S Sensitivity of Pure and Cu Doped SnO[sub 2] Single Nanowire Sensors. , 2009, , .		0
211	Positron annihilation studies of Eu and Dy doped α'-Sr2SiO4. Journal of Physics: Conference Series, 2015, 618, 012016.	0.4	0